Protein Delivery

DOI: 10.1002/ange.201302331

Two-Step Protein Self-Assembly in the Extracellular Matrix**

*Won Min Park and Julie A. Champion**

Therapeutic proteins require controlled delivery to the target tissue to maintain the local concentration over a prolonged period of time. A common approach is to delay protein release with a hydrogel matrix, which provides affinity interactions or diffusive barriers.[1] Physical entrapment of proteins in a matrix allows sustained release due to free volume, hydrodynamic drag, and obstruction effects.[2] Affinity-based approaches exploit specific binding interactions between natural[3] or engineered binding ligands[4] attached to the hydrogel matrix and therapeutic proteins. However, hydrogel-based approaches inherently involve relatively large amounts of carrier material compared to the entrapped protein therapeutic. Toxicity concerns may arise from synthetic crosslinkers or initiators used in polymerization,[5] or modification of biological polymers.[6] Biocompatibility issues, such as the foreign body response, may be present at the interface between tissue and materials.[7] Thus, a strategy that uses no or a minimal amount of carrier material is ideal, to eliminate these challenges. Herein, we demonstrate that the concept of "carrier-free" can be realized by adopting a different physical principle, protein self-assembly.

Self-assembly has been exploited as a useful tool to fabricate ordered structures from peptides[8] or proteins.[9] While much effort has been focused on fabrication of self-assembled matrices,[10] recent studies reported that protein properties, including binding avidity,[11] bioactivity,[12] and stability,[13] are modulated by protein self-assembly. In this study, we describe a self-assembly system in which proteins self-control their molecular transport in a model extracellular matrix (ECM). Engineered protein building blocks spontaneously self-assemble into particles in the ECM, become trapped, and dissociate to be released at a controlled rate. This protein self-assembly is mediated by temperature-responsive coacervation and dissociation, and by specific binding of high-affinity protein motifs under physiological conditions. Since the ECM selectively regulates microscopic motion of objects depending on their size,[14] the diffusion of protein building blocks is modulated as they form particles under non-equilibrium conditions.

The system is built from two different di-block fusion proteins. The first component (mCherry-Z_E) is constructed from a globular fluorescent protein mCherry,[15] which serves as a model for a therapeutic protein, and a glutamic acid-rich leucine zipper (Z_E). An arginine-rich leucine zipper (Z_R) and elastin-like polypeptide (ELP) comprise the second component (Z_R-ELP)[16] (Figure 1a). ELP is composed of a pentapeptide repeat derived from tropoelastin, which undergoes a temperature-responsive inverse phase transition from soluble to coacervate phase.[17] The leucine zipper motifs Z_E and Z_R form heterodimeric α-helical coiled-coils with a dissociation constant, $K_D \approx 10^{-15}$ M.[18] The fusion proteins were produced separately by using bacterial protein synthesis and purified (see the Supporting Information for experimental details).[16] In aqueous solution, Z_R-ELP showed the expected inverse phase transition as characterized by an increase in light scattering upon temperature elevation (Figure 1b). The transition temperature is dependent on the concentration of Z_R-ELP in phosphate-buffered saline (PBS containing 137 mM NaCl, pH 7.4), and Z_R-ELP at 1.9 to 24 μM formed coacervates when the solution was heated from 25 to 37 °C. Subsequent addition of mCherry-Z_E resulted in rapid binding to the Z_R-ELP coacervates within a minute (Figure S4 in the Supporting Information), showing an association rate constant of $k_{on} \approx 1.5 \times 10^5\ M^{-1}\,s^{-1}$ (Figure 1c). As elucidated by kinetic analysis and circular dichroism, Z_R/Z_R coiled-coils of Z_R-ELP simultaneously unfold during the phase transition followed by subsequent refolding of Z_R/Z_E heterodimer coiled-coils upon binding of mCherry-Z_E (see the Supporting Information).

Next, we performed the two-step self-assembly of the fusion protein components in the ECM as illustrated in Figure 1d, using a reconstituted ECM hydrogel (Matrigel) as a model for the native ECM. The inverse phase transition of soluble Z_R-ELP (25 °C) that permeated through the ECM hydrogel (37 °C) resulted in the in situ formation of coacervated particles. In the second step, mCherry-Z_E was added and bound to the particles through the high-affinity interaction between the leucine zipper motifs. As a result, we observed formation of fluorescent particulates of mCherry-Z_E/Z_R-ELP in the ECM hydrogel (Figure 2a,b) with diameters ranging from 330 nm to 1.6 μm. Interestingly, we found particulates with irregular shapes that seemed to be from incomplete coalescence of coacervated Z_R-ELP nanoparticles (Figure 2c). In aqueous solution, Z_R-ELP grows into microspheres with smooth surfaces by the coacervation–coalescence process, and the binding of mCherry-Z_E does not influence the surface morphology (Figure S4). Therefore, the observation of non-spherical particles in the ECM hydrogel

[*] W. M. Park, Prof. J. A. Champion
School of Chemical & Biomolecular Engineering
Georgia Institute of Technology
311 Ferst Dr. NW, Atlanta, GA 30332 (USA)
E-mail: julie.champion@chbe.gatech.edu
Homepage: http://champion.chbe.gatech.edu

[**] This research was supported by grants from the National Science Foundation (1032413) and GT Emory Center for Regenerative Engineering & Medicine. We acknowledge J. Park, Prof. A. Bommarius, Dr. I. Mamajanov, and Prof. N. Hud for technical assistance and Profs. K. Zhang and D. Tirrell for plasmid DNA. This work was performed in part at the GT Institute for Electronics and Nanotechnology, a member of the National Nanotechnology Infrastructure Network, which is supported by the NSF.

Supporting information for this article is available on the WWW under http://dx.doi.org/10.1002/anie.201302331.

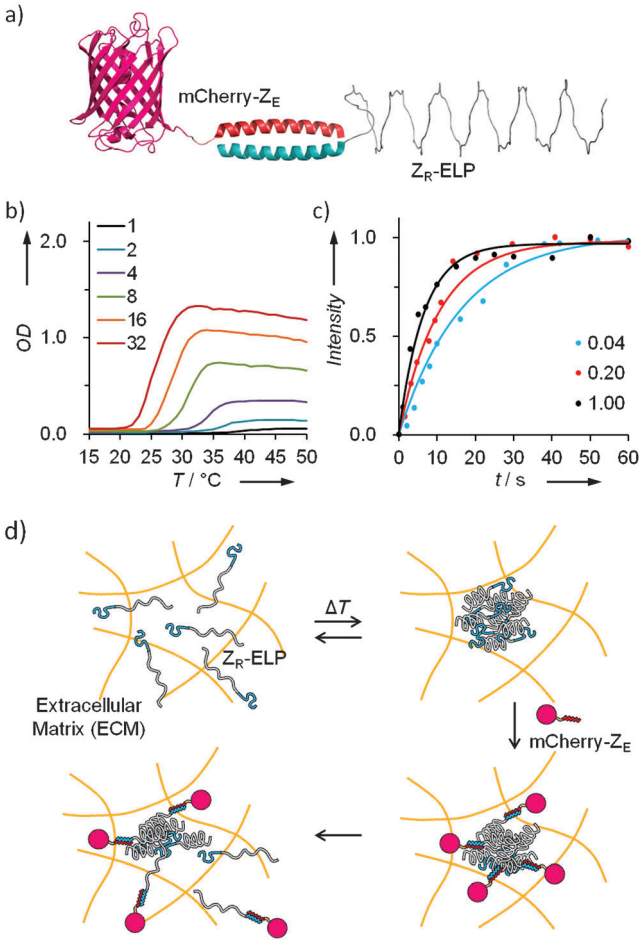

Figure 1. Protein building blocks and their self-assembly in solution phase and in ECM. a) The recombinant engineered protein building blocks, mCherry-Z_E (PDB ID for mCherry: 2H5Q) and Z_R-ELP, are produced separately, but self-assemble by formation of coiled-coils. b) The inverse phase transition of Z_R-ELP in aqueous solution: Temperature vs. optical density (OD at $\lambda = 350$ nm) measured at different concentrations of Z_R-ELP (1, 2, 4, 8, 16, 32 μM). c) The binding kinetics estimated by fluorescence intensity changes of the Z_R-ELP coacervates upon incubation with mCherry-Z_E (0.04, 0.2, 1 μM in aqueous solution). The measured intensities (dots) were fitted to a bimolecular binding model (lines) (experimental details are provided in the Supporting Information). d) Schematic illustration of the in situ self-assembly of mCherry-Z_E and Z_R-ELP in ECM.

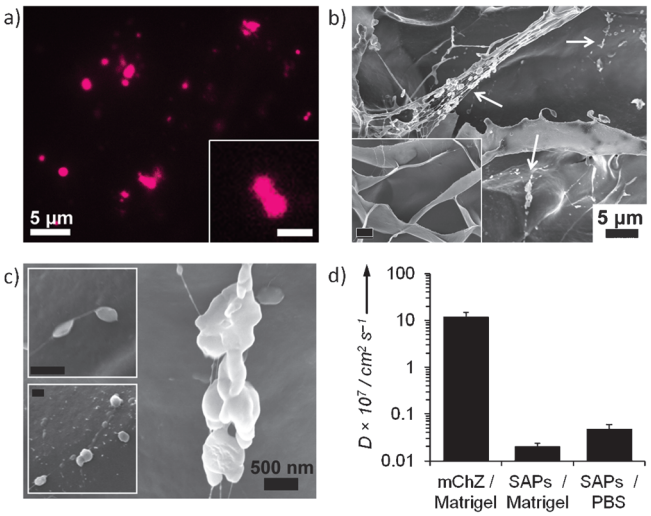

Figure 2. The mCherry-Z_E/Z_R-ELP particles that self-assembled in ECM hydrogel. a) Fluorescence micrographs of particles formed in Matrigel (inset scale bar 1 μm) b,c) Scanning electron micrographs of the particles (arrowed): the particle-embedded Matrigel was fixed with glutaraldehyde for 2 h, and freeze-dried. For comparison, the Matrigel treated with only PBS was imaged. Inset in (b), scale bar 5 μm; insets in (c), scale bars 500 nm. d) Diffusivity (D) of mCherry-Z_E (mChZ) and self-assembled particles (SAPs) in Matrigel or PBS (see the Supporting Information for details).

indicates that the coalescence of the coacervates is limited by the presence of the matrix. When Z_R-ELP was premixed with ECM solution at 4 °C and warmed up, it formed large coalesced particles (ca. 10 μm) due to initial absence of the matrix (Figure S5c). Hindered by the matrix, the self-assembled mCherry-Z_E/Z_R-ELP particles formed in the ECM hydrogel showed reduced diffusivity. Estimated from particle trajectories, the diffusivity of mCherry-Z_E/Z_R-ELP particles was 2.5-fold lower in the ECM hydrogel than in aqueous solution, and 500-fold lower than that of monomeric mCherry-Z_E in the ECM hydrogel (Figure 2d). Indeed, the in situ self-assembly resulted in entrapment of the model protein, mCherry, in the ECM hydrogel by the self-assembly process. The low diffusivity of the self-assembled mCherry-Z_E/Z_R-ELP particles is based on the hydrodynamic and steric interactions of the particles with the ECM,[19] and their insignificant electrostatic interactions with the matrix (zeta potential, $\zeta \approx -2.6$ mV)[20] allow the protein particles to be locally dynamic at a reduced mobility rather than immobilized on the matrix.

Estimated using a mathematical model,[21] the coacervation by inverse phase transition of Z_R-ELP has a rate constant, $k_c \approx 0.7\ \text{min}^{-1}$ (Figure S3a). The characteristic time for coacervation, τ_c ($\approx 1/k_c$) is ca. 90 s. The characteristic length for the system L ($\approx (D/k_c)^{0.5}$) is approximated as 100 μm if τ_c is on the same order with the characteristic time for the diffusion of dispersed Z_R-ELP, τ_d ($\approx L^2/D$). Thus, the scaling analysis accounts for the simultaneous diffusion and temperature-responsive coacervation of Z_R-ELP in the ECM. This is a reaction–diffusion system, which allows formation of self-assembled particles in a layer of thickness, L. The coacervated Z_R-ELP particles accumulated in the layer and mCherry-Z_E rapidly bound to the particles during the second step of self-assembly. We observed formation of a fluorescent layer near the ECM hydrogel–solution interface in Figure 3, and the initial concentration of Z_R-ELP controlled the amount of particles in the layer, as indicated in the fluorescence images (Figure 3b). The diffusion, coacervation, and affinity-binding of the protein building blocks in the ECM hydrogel were modeled by a one dimensional reaction–diffusion equation [Eq. (1)], where x is distance from the solution–hydrogel interface, C_i is concentration, D_i is diffusivity, and R_i is the reaction term for a protein or particle component i (see the Supporting Information for details).

$$\frac{\partial C_i}{\partial t} = D_i \frac{\partial^2 C_i}{\partial x^2} + R_i \qquad (1)$$

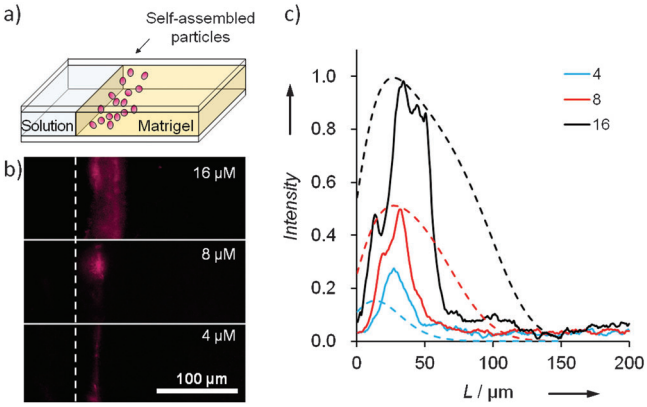

Figure 3. The layer of self-assembled particles in ECM hydrogel. a) Schematic illustration of the model system. b) Fluorescence micrographs of the layer where particles are located. c) The corresponding profiles of fluorescence intensity at distance (L) from Matrigel-solution interface: the experimental results of averaged profiles (solid) were compared with the profiles from modelling (dashed). The initial concentration of Z_R-ELP was varied (4, 8, 16 μM), and the computational modelling was performed based on reaction-diffusion equations.

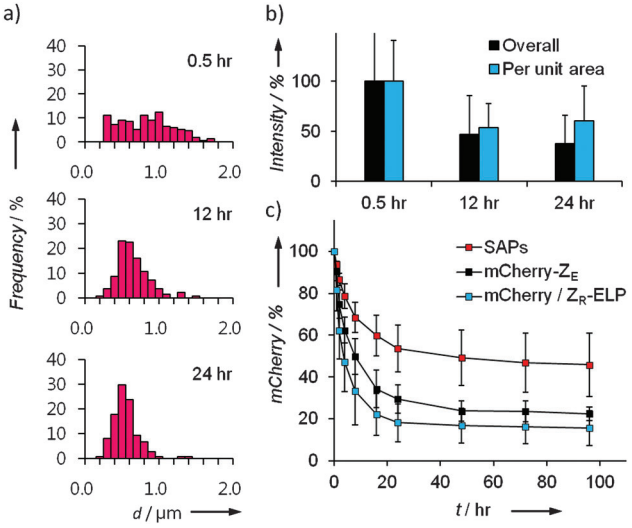

Figure 4. Dissociation of mCherry-Z_E/Z_R-ELP particles. a) Particle size distribution changes with time: the frequency of particles are indicated for corresponding diameter, *d*. b) Fluorescence intensity changes upon particle dissociation: the overall average intensity (black) and the intensity per unit area of the particles (blue). c) The release of mCherry-Z_E imbedded in Matrigel as a soluble protein (black, mCherry-Z_E) or self-assembled particles (red, SAPs), and of mCherry in the presence of Z_R-ELP (blue, mCherry/Z_R-ELP).

In our model, coacervation of Z_R-ELP from soluble proteins to particles was included in the reaction term, and the diffusivity of the particles was assumed to be constant since their size does not change significantly once they form. The modeling results were consistent with the experimental results (Figure 3c), supporting the theoretical argument of in situ self-assembly in the ECM hydrogel. Although the model does not duplicate the experimental mCherry fluorescence profile exactly, it demonstrates the ability to control the amount of mCherry-Z_E in the ECM hydrogel.

The self-assembled mCherry-Z_E/Z_R-ELP particles in the ECM hydrogel are metastable, and Z_R-ELP dissociates from the particles when the local concentration of Z_R-ELP drops below the minimum phase transition concentration (ca. 1.9 μM at 37 °C). As a result, the in situ self-assembled particles shrank over time in the ECM hydrogel. The average diameter (d) decreased from 828 ± 354 nm to 542 ± 158 nm during the first 24 h (Figure 4a). The size distribution of the particles also narrowed, indicating that the particles larger than 1 μm shrank more rapidly. The surface erosion from larger particles ($d > \approx 1$ μm) is faster than smaller particles due to the ouzo effect that smaller particles are thermodynamically favored when the concentration of Z_R-ELP decreases.[22] Concurrently, the fluorescence intensity of the particles was reduced by half after 12 h of dissociation proceeded, and there was further reduction in fluorescence to 37.8% of the initial value after 24 h (Figure 4b). The initial drop in intensity is attributed to the rapid shrinking of the large particles ($d > 1$ μm), when the rate of decrease in intensity is proportional to the shrinking rate of the particles. While the average size of particles gradually decreased, the concentration of mCherry on the particles remains approximately constant after an initial decrease of 46% in the first 12 h (calculated from the fluorescence intensity per unit area of particles). It indicates that dissociation of Z_R-ELP from the particles seems to also induce release of mCherry-Z_E/Z_R-ELP.

As suggested by the dissociation kinetics of particles, self-assembly resulted in an enhanced retention of proteins in the ECM hydrogel (Figure 4c). The in situ assembled protein building blocks in the ECM hydrogel were exposed to a reservoir of 37 °C PBS to simulate the ECM environment in vivo and generate a concentration sink to induce disassembly and diffusion. The overall retention of mCherry-Z_E with Z_R-ELP was enhanced by 100% compared to monomeric mCherry-Z_E, of which less than 30% remained in the ECM hydrogel after 24 h. Consistent with the observed dissociation kinetics in Figure 4b, dissociation of mCherry-Z_E from the self-assembled particles led to an initial clearance of mCherry-Z_E (ca. 36% loss over 12 h), which was much slower than soluble mCherry-Z_E (ca. 58% loss). Considering the drastic difference in diffusivities of soluble proteins and particles (ca. 500-fold), the controlled release of mCherry-Z_E in the ECM hydrogel should have resulted from dissociation of mCherry-Z_E from the particles. Furthermore, when mCherry without the Z_E domain was added together with Z_R-ELP in the ECM hydrogel, the release profile of mCherry/Z_R-ELP was very close to that of mCherry-Z_E alone. This result indicates that mCherry does not have specific interactions with Z_R-ELP and that the coacervates do not alter the release without the specific Z_R/Z_E interaction.

Compared to the conventional recombinant conjugation of therapeutic protein directly to ELP, the two-component system based on the leucine zippers (Z_R/Z_E) shows new features in the inverse phase transition behavior of ELP. ELP–peptide or ELP–protein conjugates have been engineered to self-assemble into nanoparticles upon the inverse phase transition,[23] which has led to remarkable progress in delivery of chemo-[24] and protein therapeutics.[25] While ELPs

of more than 60 repeats of the pentapeptide exhibit less concentration dependence, Z_R-ELP (25 repeats) undergoes inverse phase transition at relatively low temperatures (40 to 20 °C) with a strong concentration dependence (1 to 100 μM). This allows self-assembly and disassembly due to concentration gradients at 37 °C. Also, the ratio of functional protein to ELP is very flexible as they can be conjugated at different molar ratios after coacervation.

Our system is widely applicable for local delivery of protein therapeutics to diseased sites, where proteins could be topically applied or injected, and upon contact will warm to body temperature and start the assembly process. We note that this system has several advantages as a new strategy for protein delivery. First, carrier-free delivery based on protein self-assembly does not involve use of excessive synthetic or biological materials with potential biocompatibility or toxicity issues.[5–7] The self-assembling motifs, ELP and Z_R/Z_E, are derived from extra-[26] and intracellular[18] human proteins, and toxicity potential is decreased.[26,27] Furthermore, ELP has been reported to stimulate granulation in wounds,[28] which could have synergetic effects for protein delivery specifically in wound healing applications. Second, 100 % of dosed protein is spatially distributed in the ECM, and the temporal concentration gradient resulted by the dissociation of particles could yield optimal responses in applications with therapeutic proteins.[29]

In summary, we have described a protein self-assembly system where the protein components self-assemble in the ECM and become entrapped as particles, demonstrating potential as a new type of "carrier-free" protein delivery approach. Our analysis shows spontaneous diffusion–coacervation and high-affinity binding processes that mediate in situ formation of self-assembled particles that shrink and release protein in the ECM. Though demonstrated with a model fluorescent protein, this new concept is widely applicable for a variety of protein therapeutics, including growth factors and cytokines.

Received: March 19, 2013
Revised: May 15, 2013
Published online: June 20, 2013

Keywords: biomimetics · drug delivery · extracellular matrix · proteins · self-assembly

[1] N. X. Wang, H. A. von Recum, *Macromol. Biosci.* **2011**, *11*, 321 – 332.
[2] B. Amsden, *Macromolecules* **1998**, *31*, 8382 – 8395.
[3] S. E. Sakiyama-Elbert, J. A. Hubbell, *J. Controlled Release* **2000**, *69*, 149 – 158.
[4] K. Vulic, M. S. Shoichet, *J. Am. Chem. Soc.* **2012**, *134*, 882 – 885.
[5] a) B. V. Slaughter, S. S. Khurshid, O. Z. Fisher, A. Khademhosseini, N. A. Peppas, *Adv. Mater.* **2009**, *21*, 3307 – 3329; b) J. S. Temenoff, H. Shin, D. E. Conway, P. S. Engel, A. G. Mikos, *Biomacromolecules* **2003**, *4*, 1605 – 1613.
[6] T. Kean, M. Thanou, *Adv. Drug Delivery Rev.* **2010**, *62*, 3 – 11.
[7] J. M. Anderson, A. Rodriguez, D. T. Chang, *Semin. Immunol.* **2008**, *20*, 86 – 100.
[8] S. Zhang, *Nat. Biotechnol.* **2003**, *21*, 1171 – 1178.
[9] J. C. Sinclair, K. M. Davies, C. Venien-Bryan, M. E. M. Noble, *Nat. Nanotechnol.* **2011**, *6*, 558 – 562.
[10] a) C. T. S. Wong Po Foo, J. S. Lee, W. Mulyasasmita, A. Parisi-Amon, S. C. Heilshorn, *Proc. Natl. Acad. Sci. USA* **2009**, *106*, 22067 – 22072; b) W. Shen, K. Zhang, J. A. Kornfield, D. A. Tirrell, *Nat. Mater.* **2006**, *5*, 153 – 158; c) A. Bella, S. Ray, M. Shaw, M. G. Ryadnov, *Angew. Chem.* **2012**, *124*, 443 – 446; *Angew. Chem. Int. Ed.* **2012**, *51*, 428 – 431; d) S. Koutsopoulos, L. D. Unsworth, Y. Nagai, S. Zhang, *Proc. Natl. Acad. Sci. USA* **2009**, *106*, 4623; e) S. Toledano, R. J. Williams, V. Jayawarna, R. V. Ulijn, *J. Am. Chem. Soc.* **2006**, *128*, 1070 – 1071.
[11] A. J. Simnick, C. A. Valencia, R. Liu, A. Chilkoti, *ACS Nano* **2010**, *4*, 2217 – 2227.
[12] M. R. Diehl, K. Zhang, H. J. Lee, D. A. Tirrell, *Science* **2006**, *311*, 1468 – 1471.
[13] J. C. T. Carlson, S. S. Jena, M. Flenniken, T.-f. Chou, R. A. Siegel, C. R. Wagner, *J. Am. Chem. Soc.* **2006**, *128*, 7630 – 7638.
[14] O. Lieleg, K. Ribbeck, *Trends Cell Biol.* **2011**, *21*, 543 – 551.
[15] X. Shu, N. C. Shaner, C. A. Yarbrough, R. Y. Tsien, S. J. Remington, *Biochemistry* **2006**, *45*, 9639 – 9647.
[16] K. Zhang, A. Sugawara, D. A. Tirrell, *ChemBioChem* **2009**, *10*, 2617 – 2619.
[17] D. W. Urry, T. L. Trapane, K. U. Prasad, *Biopolymers* **1985**, *24*, 2345 – 2356.
[18] J. R. Moll, S. B. Ruvinov, I. Pastan, C. Vinson, *Protein Sci.* **2001**, *10*, 649 – 655.
[19] T. Stylianopoulos, M.-Z. Poh, N. Insin, M. G. Bawendi, D. Fukumura, L. L. Munn, R. K. Jain, *Biophys. J.* **2010**, *99*, 1342 – 1349.
[20] O. Lieleg, R. M. Baumgärtel, A. R. Bausch, *Biophys. J.* **2009**, *97*, 1569 – 1577.
[21] J. T. Cirulis, C. M. Bellingham, E. C. Davis, D. Hubmacher, D. P. Reinhardt, R. P. Mecham, F. W. Keeley, *Biochemistry* **2008**, *47*, 12601 – 12613.
[22] S. A. Vitale, J. L. Katz, *Langmuir* **2003**, *19*, 4105 – 4110.
[23] a) T. A. T. Lee, A. Cooper, R. P. Apkarian, V. P. Conticello, *Adv. Mater.* **2000**, *12*, 1105 – 1110; b) M. R. Dreher, A. J. Simnick, K. Fischer, R. J. Smith, A. Patel, M. Schmidt, A. Chilkoti, *J. Am. Chem. Soc.* **2008**, *130*, 687 – 694; c) W. Kim, J. Thévenot, E. Ibarboure, S. Lecommandoux, E. L. Chaikof, *Angew. Chem.* **2010**, *122*, 4353 – 4356; *Angew. Chem. Int. Ed.* **2010**, *49*, 4257 – 4260.
[24] a) J. A. MacKay, M. Chen, J. R. McDaniel, W. Liu, A. J. Simnick, A. Chilkoti, *Nat. Mater.* **2009**, *8*, 993 – 999; b) D. Y. Furgeson, M. R. Dreher, A. Chilkoti, *J. Controlled Release* **2006**, *110*, 362 – 369.
[25] a) M. F. Shamji, H. Betre, V. B. Kraus, J. Chen, A. Chilkoti, R. Pichika, K. Masuda, L. A. Setton, *Arthritis Rheum.* **2007**, *56*, 3650 – 3661; b) M. F. Shamji, J. Chen, A. H. Friedman, W. J. Richardson, A. Chilkoti, L. A. Setton, *J. Controlled Release* **2008**, *129*, 179 – 186.
[26] D. W. Urry, T. M. Parker, M. C. Reid, D. C. Gowda, *J. Bioact. Compat. Polym.* **1991**, *6*, 263 – 282.
[27] W. Shen, PhD thesis, California Institute of Technology (USA), **2005**.
[28] P. Koria, H. Yagi, Y. Kitagawa, Z. Megeed, Y. Nahmias, R. Sheridan, M. L. Yarmush, *Proc. Natl. Acad. Sci. USA* **2011**, *108*, 1034 – 1039.
[29] E. A. Silva, D. J. Mooney, *Biomaterials* **2010**, *31*, 1235 – 1241.

